arXiv:1602.01044v1 [cond-mat.quant-gas] 2 Feb 2016

Stable core symmetries and confined textures for a vortex line in a spinor Bose-Einstein condensate

Magnus O. Borgh,[1] Muneto Nitta,[2] and Janne Ruostekoski[1]

[1] *Mathematical Sciences, University of Southampton, SO17 1BJ, Southampton, UK*
[2] *Department of Physics, and Research and Education Center for Natural Sciences, Keio University, Hiyoshi 4-1-1, Yokohama, Kanagawa 223-8521, Japan*

(Dated: February 3, 2016)

We show how a singly quantized vortex can exhibit energetically stable defect cores with different symmetries in an atomic spin-1 polar Bose-Einstein condensate, and how a stable topologically nontrivial Skyrmion texture of lower dimensionality can be confined inside the core. The core isotropy and the stability of the confined texture are sensitive to Zeeman level shifts. The observed structures have analogies, respectively, in pressure-dependent symmetries of superfluid liquid ^{3}He vortices and in the models of superconducting cosmic strings.

PACS numbers: 67.85.Fg, 03.75.Mn, 03.75.Lm, 11.27.+d,

Topological defects and textures cannot be removed from the system by any continuous local transformation, rendering them inherently robust and stable. Their topological properties are universal throughout nature from high-energy physics and cosmology to superfluids and liquid crystals [1]. Defects and textures in different physical systems can therefore frequently be characterized by generic effective theories that are less sensitive to underlying microscopic interactions between constituent particles. Here the highly accessible atomic systems provide unprecedented opportunities to act as simulators [2, 3] of phenomena in condensed-matter systems, high-energy physics and cosmology. For instance, defect formation in nonequilibrium phase transitions using the Kibble-Zurek mechanism [4, 5] has been realized experimentally in both scalar and spinor atomic Bose-Einstein Condensates (BECs) [6–9] and the creation of black-hole analogs has been proposed theoretically [10]. Studies of cosmological phenomena are also known in superfluid liquid ^{3}He [11–13], despite their less flexible experimental control and more indirect detection methods.

Recent experimental progress in the studies of spinor-BEC topological defects and textures has culminated in the controlled preparation [14, 15] of the atomic superfluid analogs of Dirac [16–18] and 't Hooft-Polyakov [19, 20] monopoles, coreless textures [21–24], and *in situ* observation of the spontaneous breaking of core axisymmetry of a singly quantized vortex. In the last case the vortex with an initially isotropic core split into two half-quantum vortices [25], confirming the theoretical prediction [26].

In this Letter, we demonstrate that the stable core of a singly quantized spin-1 vortex, which was studied in the recent experiments [25], can exhibit different axisymmetries that continuously vary with imposed Zeeman shifts, and that the vortex core can host energetically stable, topologically nontrivial confined spin textures. The coexistence of energetically stable vortex cores exhibiting different symmetries is analogous to the vortex cores of different isotropies encountered in superfluid liquid ^{3}He [27–29]. The confined stable spin texture inside the vortex corresponds to a continuous one-dimensional (1D) baby Skyrmion [30].

Defects or textures of lower dimensionality that are confined inside the cores of singular host defects form elegant topological objects. Here we show that a 1D texture trapped inside the core of a singular vortex line can be prepared and energetically stabilized by engineering spatial profiles of the Zeeman shifts. These fix the boundary conditions on the spin texture, ensuring that it corresponds to a 1D baby Skyrmion with a nontrivial 1/2 topological charge, forming an analogy to the Witten model of a scalar field winding along a cosmic string defect line [31]. A closed loop of such a string is a cosmic vorton [32]. Although the analogs of vortons and 3D Skyrmions [33] have been actively investigated in atomic BECs [34–39], their experimental preparation has proved to be challenging due to their inherently complex 3D structure—complications that could be avoided by the simple preparation protocol of the confined 1D texture we propose here. Aside from their interest in cosmology, lower-dimensional Skyrmions confined by domain walls or singular line defects appear also in high-energy physics [40], e.g., as the stable state of confined monopoles in quantum chromodynamics (QCD) [41–44].

In the mean-field theoretical model the condensate wave function Ψ is represented by the atomic density $n = \Psi^\dagger\Psi$ and a three-component spinor ζ, such that

$$\Psi(\mathbf{r}) = \sqrt{n(\mathbf{r})}\zeta(\mathbf{r}) = \sqrt{n(\mathbf{r})}\begin{pmatrix}\zeta_+(\mathbf{r})\\ \zeta_0(\mathbf{r})\\ \zeta_-(\mathbf{r})\end{pmatrix}, \quad \zeta^\dagger\zeta = 1. \quad (1)$$

The expectation value $\langle\hat{\mathbf{F}}\rangle$ of the spin operator gives the local condensate spin. The Hamiltonian density is then [45]

$$\mathcal{H} = h_0 + \frac{c_0}{2}n^2 + \frac{c_2}{2}n^2|\langle\hat{\mathbf{F}}\rangle|^2 - pn\langle\hat{F}_z\rangle + qn\langle\hat{F}_z^2\rangle\,, \quad (2)$$

where $h_0 = (\hbar^2/2m)\left|\nabla\Psi\right|^2 + (m\omega^2/2)(x^2+y^2+z^2/4)n$, assuming a slightly prolate trap. Linear and quadratic Zeeman shifts are represented by p and q. The interaction strengths are given by $c_0 = 4\pi\hbar^2(2a_2+a_0)/3m$ and $c_2 = 4\pi\hbar^2(a_2-a_0)/3m$, where a_f is the s-wave scattering length in the spin-f channel.

There are several theoretical studies of vortex structures in spin-1 BECs [26, 46–59] that result from the rich order parameter space supported by the Hamiltonian (2). Here we assume $c_0, c_2 > 0$ (we take the value $c_0/c_2 \simeq 28$ for ^{23}Na [60]), in which case the interaction energy favors the polar phase with $|\langle\hat{\mathbf{F}}\rangle| = 0$ (for a uniform system). The order parameter ζ is then fully specified by the condensate phase τ and an unoriented unit vector $\hat{\mathbf{d}}$ [30, 47], exhibiting *nematic order*: $\zeta(\tau,\hat{\mathbf{d}}) = \zeta(\tau+\pi,-\hat{\mathbf{d}})$. Vortices may then be characterized by the winding of both τ and $\hat{\mathbf{d}}$, where, however, only τ contributes to the superfluid current and determines the topological charge. The nematic order leads to the existence of half-quantum vortices where a $\pm\pi$ winding in τ is compensated by a $\hat{\mathbf{d}} \to -\hat{\mathbf{d}}$ rotation [47]. These were recently observed in experiment [25]. Note that the name half-quantum vortex is sometimes used also in two-component condensates, e.g., of exciton-polaritons [61, 62], where, however, the structure does not arise from nematic order as in superfluid liquid ^{3}He [27, 28], liquid crystals [63], or atomic BECs, but is more reminiscent of a topologically very different coreless vortex [64]. In the spin-1 BEC, the nematic order also allows several different ways of forming a vortex with a given topological charge (see for example Refs. [45, 65] for detailed presentations of the basic vortices). Here we consider a singly quantized vortex with an associated 2π winding of $\hat{\mathbf{d}}$. This may be written as

$$\zeta = \frac{1}{\sqrt{2}}\begin{pmatrix} -\sin\beta \\ \sqrt{2}e^{i\varphi}\cos\beta \\ e^{i2\varphi}\sin\beta \end{pmatrix}, \tag{3}$$

such that $\hat{\mathbf{d}} = \cos\varphi\sin\beta\hat{\mathbf{x}} + \sin\varphi\sin\beta\hat{\mathbf{y}} + \cos\beta\hat{\mathbf{z}}$ and $\tau = \varphi$ [47], where φ is the azimuthal angle and β the angle between $\hat{\mathbf{d}}$ and the z axis (taken to be constant).

We numerically minimize the mean-field energy, Eq. (2), in the frame rotating at frequency Ω (chosen to keep the vortex stable) around the z axis, for different core structures of the singly quantized polar vortex. This is done by propagating the Gross-Pitaevskii equations obtained from (2) in imaginary time using the split-step algorithm [66]. We choose the nonlinearity $Nc_0 = 5000\hbar\omega\ell^3$ [$\ell \equiv (\hbar/m\omega)^{1/2}$]. For ^{23}Na scattering lengths [60], this yields $N\omega^{1/2} \simeq 7.5\times10^6\mathrm{s}^{-1/2}$ between the number of atoms and the trap frequency. For example, in a typical trap with $\omega = 2\pi\times10$Hz, this corresponds to $N \simeq 10^6$ atoms. We consider initial states constructed from Eq. (3), and determine the relaxed state in the presence of uniform and nonuniform Zeeman shifts p and q.

In addition to the Zeeman shifts arising from external magnetic fields, an AC Stark shift corresponding to a highly tunable quadratic level shift may be induced by combining a static magnetic field with a microwave dressing field [67]. This method has already been applied to the study of spin textures [68]. Level shifts may also be induced by lasers [69], which can allow for increased spatial control.

When $c_0 > c_2$, it is energetically favorable for a polar vortex to exhibit a core with nonzero superfluid density where the BEC reaches the FM phase at the line singularity [20, 26, 57]. For weak Zeeman shifts, this mechanism was predicted to lead to breaking of axisymmetry in the vortex core by splitting of the singly quantized vortex into a pair of half-quantum vortices, exhibiting FM cores whose spins anti-align, and preserving the topology away from the core region [26, 30]. The theoretical prediction was confirmed by the very recent *in situ* observation of the dissociation process [25], where isotropic vortices were prepared by means of trap and spin rotation.

Here we find that the symmetry of the vortex core is sensitive to the tunable Zeeman shifts. In particular, sufficiently large (spatially uniform) p and q may partially or completely restore the axial symmetry of the vortex core. This is illustrated in Fig. 1, showing $|\langle\hat{\mathbf{F}}\rangle|$ at its local minimum between the singular lines, providing a measure for the degree of core splitting, along with examples of stable vortex core structures exhibiting different axisymmetry. A positive quadratic shift favors population of the ζ_0 component and acts to compress the core region. However, this still exhibits two distinct singular lines with antialigning spins, forcing the wave function to the polar phase between them, also as q increases. If in addition p is sufficiently large, the spins bend towards the z direction, and since the spins then do not antialign, a contiguous nonpolar core region can form. As p and q increase, the half-quantum vortex cores gradually merge, forming a nonpolar core with broken axisymmetry, until the splitting is suppressed entirely as $p \gtrsim 0.1\hbar\omega$ and $q \gtrsim 0.5\hbar\omega$ [cf. Fig. 1(d)], leading to a single, axisymmetric FM core. When p approaches $0.2\hbar\omega$ and q comes close to the trap energy, the density in the vortex core is decreased, and the population of ζ_- suppressed.

The existence of rich vortex core topologies has been predicted in superfluid liquid ^{3}He [27, 28]. Owing to the flexibility of experimental preparation of atomic spinor gases and the atomic physics technology for direct detection and control, the studies of vortex core structures could be less challenging in atomic BECs. The coexistence of stable vortices with different core symmetries in a spin-1 BEC is similar to that observed for B-phase vortices in superfluid liquid ^{3}He as the pressure is varied [29, 70–72]. At high pressure, an axially symmetric vortex core where the A phase appears on the singular line [70] has the lower energy [71, 72]. However, at lower pressure, energy is instead minimized by the "double-core vortex" [71, 72], in which the extended core region corresponds to two half-quantum vortices in the planar phase.

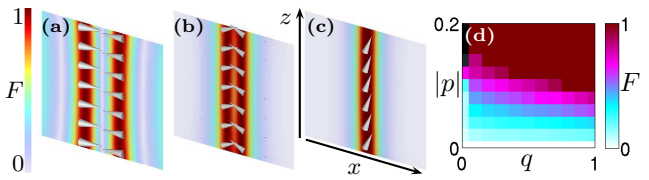

FIG. 1. (Color online) (a)-(c) Spin vector (cones) and magnitude (color gradient) in stable vortex cores of different symmetries: For weak Zeeman shifts, the broken axisymmetry of the vortex cores displays half-quantum vortices with antialigning spins in the FM cores. The core symmetry is gradually restored as level shifts increase. Panels cover $|x| \leq 3.9$, $|z| \leq 3.6$ (a) $p = q = 0.0$, (b) $p = 0.1\hbar\omega, q = 0.4\hbar\omega$ and (c) $p = 0.1\hbar\omega, q = 0.9\hbar\omega$. Trap rotation frequency $\Omega = 0.26\omega$. (d) Spin magnitude $F = |\langle\hat{\mathbf{F}}\rangle|$ at the local minimum between the singular lines ($F = 1$ is the isotropic limit; black indicates pair not stable) as function of p and q (units of $\hbar\omega$).

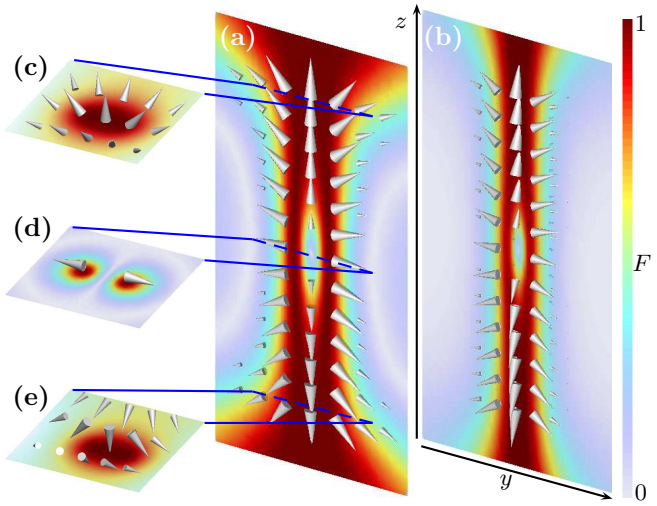

FIG. 2. (Color online) (a)-(b) Spin vector (cones) and magnitude $F = |\langle\hat{\mathbf{F}}\rangle|$ (color gradient) in the energetically stable, confined spin texture of a 1D baby Skyrmion. Boundary conditions are enforced by spatially nonuniform linear Zeeman shift, interpolating linearly between $p = \pm 0.2\hbar\omega$ over $|z| \leq 1\ell$ for $\Omega = 0.25\omega$, with (a) $q = 0.1\hbar\omega$ and (b) $q = 0.4\hbar\omega$. The splitting instability of the vortex is suppressed, except in a small region around $z = 0$. Panels cover $|y| \leq 4.9$, $|z| \leq 7.5$. (c)-(e) Cuts perpendicular to the vortex line, showing radial and cross disgyration connecting via the split region.

In contrast to the continuously variable vortex-core symmetry in the spinor BEC, the transition between the two core structures in ^{3}He is first order [28, 71, 72].

So far we have shown that spatially uniform Zeeman shifts can lead to energetically stable vortex cores of different symmetries. We now proceed to show that nontrivial, lower-dimensional textures confined inside vortex cores can be engineered and stabilized by designing Zeeman shifts with a *nonuniform* spatial profile. In doing so, we consider again the singly quantized vortex in Eq. (3). However, we now make the additional assumption that the linear Zeeman shift has an engineered, nonuniform spatial dependence $p(z)$, with different sign for positive and negative z. The Zeeman energy strives to orient the spins in opposite directions in the two parts of the vortex core. For simplicity, we assume a linear gradient in p between limits $\pm|p_{\rm lim}|$ reached well within the extent of the gas. If $|p_{\rm lim}|$ is sufficiently large, the spin bending energy may be overcome and a nontrivial spin texture can be stabilized. We further take the (spatially uniform) quadratic shift $q > 0$ to be sufficiently large that the splitting instability of the vortex is strongly suppressed. The ground-state solution in the uniform system for the chosen parameters is the polar phase [45, 73, 74]. We numerically minimize the energy in the rotating frame.

A typical example of the resulting core structure is shown in Fig. 2, where an energetically stable, continuous spin texture has emerged in the vortex core. Away from the origin, the axial symmetry of the vortex core is not broken. Around the origin, however, the vortex splits into two separate cores over a short distance as p switches sign. The size of this region is insensitive to a very sharp p gradient but becomes more pronounced if the variation is slow compared with the spin healing length $\xi_F = \hbar/(2m|c_2|n)^{1/2}$. As the quadratic level shift q is increased, the unsplit vortex core of the singly quantized vortex becomes more sharply defined and more axially symmetric, and the spin texture consequently increasingly 1D.

The spin-vector field inside the vortex core relaxes into a continuous texture where the condensate spin asymptotically orients in opposite directions for positive and negative z. (Note that the spin texture in a plane perpendicular to the vortex line changes from radial to cross disgyration across the origin. This is possible due to the local splitting of the core.) One may then think of the engineered linear Zeeman shift as imposing fixed boundary conditions on the spin in the relaxed state due to an energetic constraint. The FM core provides an energetic confinement for the spin texture, as $|\langle\hat{\mathbf{F}}\rangle|$ quickly falls off towards zero outside it. The spin texture along each singular line, where $|\langle\hat{\mathbf{F}}\rangle| = 1$, may then be viewed as a 1D baby Skyrmion, exhibiting a nonsingular, nontrivial winding of the spin vector from $-\hat{\mathbf{z}}$ to $\hat{\mathbf{z}}$ (cf. schematic illustration in Fig. 3).

The 1D baby-Skyrmion texture constitutes a lower-dimensional version of 3D Skyrmions, which are 3D localized particlelike textures [34], or 2D baby Skyrmions, which are 2D fountainlike textures (Anderson-Toulouse-Chechetkin coreless vortices [75, 76]). The winding of the 1D Skyrmion texture inside the vortex line is similar to the winding of a scalar field along a defect line in the Witten model of superconducting cosmic strings [31]. Closed loops of such strings constitute cosmic vortons, which are closely related to the 3D Skyrmion [32]. While attracting

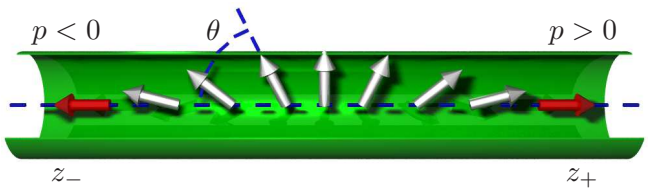

FIG. 3. (Color online) Schematic illustration of the 1D half-Skyrmion spin texture (arrows) along a vortex core (cylinder). The angle θ between the spin vector and the vortex line plays the role of an S^1 order parameter. Red (dark gray) arrows indicate fixed boundary conditions leading to a $W = 1/2$ 1D Skyrmion charge.

considerable theoretical interest, analogs of vortons and Skyrmions have proved difficult to realize in experiment due to the complicated 3D texture. Here our proposed method for creating a 1D Skyrmion could provide an experimentally simpler analog.

The 1D spin texture can be characterized by a winding number

$$W = \frac{1}{2\pi}\int_{z_-}^{z_+} dz \frac{d\theta}{dz}, \tag{4}$$

where θ is the angle between the spin vector and the vortex line (see Fig. 3), and the integration interval covers the whole texture. W is then the number of times the spin winds around the corresponding order-parameter space S^1, and consequently takes an integer value when the asymptotic spin vector is the same at both ends of the texture. Whenever the boundary conditions are fixed, for example by energetic constraints, W represents a conserved topological charge. Here the boundary conditions imposed by the Zeeman energy are $\theta(z \to z_-) = 0$ and $\theta(z \to z_+) = \pi$, and we may thus ascribe a charge $W = 1/2$ to the texture in Fig. 2.

Similar 1D baby-Skyrmion textures along vortex lines appear in supersymmetric extensions of QCD [40]. For example, a confined 1D Skyrmion texture forms the stable state of a confined monopole [41–44]. In this case a spin field $\mathbf{n}$ is confined to the core of a vortex line. For the boundary conditions $n_z(z \to +\infty) = +1$ and $n_z(z \to -\infty) = -1$, analogous to those given by the Zeeman shifts in the atomic system, $\mathbf{n}$ takes the form $n_z = \cos\theta, n_x = \sin\theta$, where $\theta = 2\arctan\{\exp[\sqrt{2}m(z - z_0)]\}$ is a sine-Gordon kink solution with the kink at z_0. The corresponding $\mathbf{n}$ texture is then similar to Fig. 3 and to the confined-Skyrmion spin texture found numerically for the spinor BEC in Fig 2.

Our results demonstrate that energy relaxation under engineered Zeeman shift may be used to experimentally realize the different core symmetries and the confined baby-Skyrmion texture in the atomic spinor BEC. The laser stirring in combination with a spin rotation used to generate the singly quantized vortices in the recent core-splitting experiment [25] could be directly applied to create the vortices. Alternatively, singular vortices can be prepared using phase-imprinting techniques [22, 64, 77–79]. The core structure can subsequently be measured *in situ* by phase-contrast imaging, as used in the recent vortex experiment [25], or detected by ballistic expansion and separation of the spinor components.

In conclusion, in a system analogous to recent spinor experiments [25] we have demonstrated the existence of different vortex core topologies and composite defects where a stable lower-dimensional Skyrmion texture is confined inside the core of a vortex line. For a singular spin-1 vortex line the spontaneous breaking of the axisymmetry of the vortex core was experimentally observed [25]. We found that the core isotropy is sensitive to tunable Zeeman shifts leading to the coexistence of different stable vortex core symmetries, where the broken symmetry could be continuously restored by experimental control. This could open up possibilities for the studies of rich vortex core topologies previously predicted for superfluid liquid ^{3}He [27, 28]. Adding spatially nonuniform Zeeman shifts results in a stable nonsingular 1D Skyrmion spin texture that is confined inside the singular vortex line core. Remarkably, this confined texture emerges from a continuous spin-1 condensate with only a single chemical potential everywhere in space. The structure is analogous to the models of superconducting cosmic strings, and is also reminiscent of confined textures in QCD. In the cosmological models a scalar field winding along a cosmic string defect is considered to provide additional stability for the string that could be further investigated in the atomic system. In the atomic superfluid a rapid rotation leads to a vortex lattice with a Skyrmion spin texture trapped along each vortex line, which can be used in studies of collective interactions between the lower-dimensional confined textures. Moreover, when a spatially nonuniform Zeeman shift profile is combined with phase transition dynamics involving spontaneous defect formation [6–9], we can also envisage simplified simulation models for superconducting cosmic string formation scenarios, where the Kibble-Zurek mechanism would involve an internal defect structure.

We acknowledge financial support from the EPSRC. The work of M. N. is supported in part by a Grant-in-Aid for Scientific Research on Innovative Areas "Topological Materials Science" (KAKENHI Grant No. 15H05855) and "Nuclear Matter in Neutron Stars Investigated by Experiments and Astronomical Observations" (KAKENHI Grant No. 15H00841) from the the Ministry of Education, Culture, Sports, Science (MEXT) of Japan, by the Japan Society for the Promotion of Science (JSPS) Grant-in-Aid for Scientific Research (KAKENHI Grant No. 25400268), and by the MEXT-Supported Program for the Strategic Research Foundation at Private Universities "Topological Science" (Grant No. S1511006). We acknowledge the use of the IRIDIS High Performance Computing Facility at the University of Southampton.

M. N. thanks the University of Southampton for warm hospitality during which this project took shape.

Supplemental Material

In this Supplemental Material we provide additional discussion of the breaking of axisymmetry in the core of a stable singly quantized vortex in the polar phase of the spin-1 BEC. We also give a brief overview of the Skyrmion textures in different dimensions.

BREAKING OF VORTEX-CORE AXISYMMETRY

In the main text, we show that the singly quantized vortex without internal structure can exhibit different, energetically stable core symmetries as the (spatially uniform) Zeeman shifts are varied. When the level shifts are weak, energy relaxation leads to spontaneous breaking of axial symmetry in the core, splitting the vortex into two half-quantum vortices, as predicted in Ref. [26]. This splitting of the vortex core was recently experimentally observed for a ^{23}Na spin-1 BEC of 3.5×10^6 atoms in an oblate trap with $(\omega_x,\omega_y,\omega_z)=2\pi\times(4.2,5.3,480)$ Hz [25]. In this experiment, singly quantized vortices were created in a condensate initially occupying only the $m=0$ Zeeman level. A spin rotation is then applied by tuning the quadratic Zeeman shift (induced using microwave dressing [67]) to transfer population to the $m=\pm1$ levels. After the spin rotation, the vortices are observed to split into half-quantum vortex pairs with opposite core spin polarization. The resulting half-quantum vortices were identified by *in situ* imaging [25], in which spin-dependent phase-contrast imaging is used to map out the condensate magnetization. The oppositely magnetized FM cores of the half-quantum vortices can then be discerned.

The breaking of axisymmetry and splitting of the singly quantized vortex is made possible by the (uniaxial) *nematic order* exhibited by the polar phase of the spin-1 BEC, which allows the existence of half-quantum vortices. The polar order parameter may be expressed in terms of a condensate phase τ and a unit vector $\hat{\mathbf{d}}$ as [47]

$$\zeta=\frac{e^{i\tau}}{\sqrt{2}}\begin{pmatrix}d_x+id_y\\ \sqrt{2}d_z\\ d_x-id_y\end{pmatrix}=\frac{e^{i\tau}}{\sqrt{2}}\begin{pmatrix}-e^{-i\alpha}\sin\beta\\ \sqrt{2}\cos\beta\\ e^{i\alpha}\sin\beta\end{pmatrix}. \quad \text{(S1)}$$

(In the last expression $\hat{\mathbf{d}}$ has been parametrized in terms of azimuthal and polar angles α and β, for later convenience). Note that $\zeta(\tau,\hat{\mathbf{d}})=\zeta(\tau+\pi,-\hat{\mathbf{d}})$. These two states must therefore be identified, and the vector $\hat{\mathbf{d}}$ is understood as an unoriented *nematic axis*. Rotations of $\hat{\mathbf{d}}$ do not contribute to the superfluid flow, making it possible to form a vortex carrying half a quantum of circulation by letting a π winding of τ around the vortex line be accompanied by a $\hat{\mathbf{d}}\to-\hat{\mathbf{d}}$ rotation of the nematic axis, keeping the order parameter single-valued. For example, taking $d_z=0$ for simplicity, a half-quantum vortex can be written as

$$\zeta=\frac{e^{i\varphi/2}}{\sqrt{2}}\begin{pmatrix}-e^{-i\varphi/2}\\ 0\\ e^{i\varphi/2}\end{pmatrix}=\frac{1}{\sqrt{2}}\begin{pmatrix}-1\\ 0\\ e^{i\varphi}\end{pmatrix}, \quad \text{(S2)}$$

where φ is the azimuthal coordinate around the vortex line. Nematic order also gives rise to half-quantum vortices in, e.g., the A phase of superfluid liquid ^{3}He [28], and to π-disclinations in nematic liquid crystals [63]. The name is also sometimes used in the context of exciton-polariton condensates in reference to a vortex with a π rotation of linear polarization of the photon component [61, 62]. This does not, however, arise from nematic order, but is more reminiscent of a topologically very different coreless vortex in a two-component BEC [64].

We can now understand the splitting of the singly quantized vortex given by Eq. (3) of the main text as

$$\frac{e^{i\varphi}}{\sqrt{2}}\begin{pmatrix}-e^{-i\varphi}\sin\beta\\ \sqrt{2}\cos\beta\\ e^{i\varphi}\sin\beta\end{pmatrix}\to \frac{e^{i\varphi_1/2}}{\sqrt{2}}\begin{pmatrix}-e^{-i\varphi_1/2}\sin\beta\\ \sqrt{2}\cos\beta\\ e^{i\varphi_1/2}\sin\beta\end{pmatrix}\oplus\frac{e^{i\varphi_2/2}}{\sqrt{2}}\begin{pmatrix}-e^{-i\varphi_2/2}\sin\beta\\ \sqrt{2}\cos\beta\\ e^{i\varphi_2/2}\sin\beta\end{pmatrix}. \quad \text{(S3)}$$

Here the spinors on the right-hand side represent half-quantum vortices [cf. Eq. (S2)]. In these, $\varphi_{1,2}$ are the azimuthal angles relative to each vortex line, and the spinors describe the wave function locally around each vortex core. Away from the core region, the wave function still corresponds to the original singly quantized vortex. (Note that $\oplus$ here indicates the addition of topological defects.)

SKYRMIONS AND BABY SKYRMIONS

Nonsingular textures may be topologically nontrivial by considering maps from a compactified real space to the compact order-parameter space. When the order parameter reaches the same value everywhere sufficiently far away from the (particlelike) texture, the entire boundary enclosing the texture may be identified and the volume in $\mathbb{R}^3$ becomes topologically S^3 (a unit sphere in four dimensions). One may then think of the $S^3\to S^3$ map as distributing (an integer number of copies of) the full order-parameter space over the compactified real space. The corresponding nontrivial textures are the 3D Skyrmions [80]. Analogous structures may be constructed in a two-component BEC [34].

An S^2 order-parameter space, may similarly be distributed over a (2D) real-space surface with fixed, uniform boundary conditions (corresponding to an $S^2 \to S^2$ map). Such a 2D Skyrmion is commonly referred to as a (2D) "baby Skyrmion", being the topologically lower-dimensional analog of the full 3D Skyrmion, and may be realized as a coreless vortex [21–24]. The dimensionality of the baby Skyrmion may be further reduced by considering an S^1 order parameter. For uniform boundary conditions such that 1D space can be compactified to S^1, the resulting $S^1 \to S^1$ map defines a 1D baby Skyrmion. In our system a ferromagnetic spin texture confined inside the core of a vortex line exhibits fixed boundary conditions. As the boundary conditions are twisted (the orientation of the spin vector differs by π in the two ends of the vortex line, the 1D Skyrmion winding number is equal to 1/2. Any further winding of the spin texture would lead to higher Skyrmion winding numbers.

[1] L. M. Pismen, *Vortices in Nonlinear Fields* (Oxford University Press, Oxford, 1999).
[2] I. Bloch, J. Dalibard, and S. Nascimbne, Nat Phys **8**, 267 (2012).
[3] I. M. Georgescu, S. Ashhab, and F. Nori, Rev. Mod. Phys. **86**, 153 (2014).
[4] T. W. B. Kibble, J. Phys. A: Mat. Gen. **9**, 1387 (1976).
[5] W. H. Zurek, Nature **317**, 505 (1985).
[6] L. E. Sadler, J. M. Higbie, S. R. Leslie, M. Vengalattore, and D. M. Stamper-Kurn, Nature **443**, 312 (2006).
[7] C. N. Weiler, T. W. Neely, D. R. Scherer, A. S. Bradley, M. J. Davis, and B. P. Anderson, Nature **455**, 948 (2008).
[8] G. Lamporesi, S. Donadello, S. Serafini, F. Dalfovo, and G. Ferrari, Nat Phys **9**, 656 (2013).
[9] N. Navon, A. L. Gaunt, R. P. Smith, and Z. Hadzibabic, Science **347**, 167 (2015).
[10] L. J. Garay, J. R. Anglin, J. I. Cirac, and P. Zoller, Phys. Rev. Lett. **85**, 4643 (2000).
[11] G. E. Volovik, *The Universe in a Helium Droplet* (Oxford University Press, 2003).
[12] C. Bäuerle, Y. M. Bunkov, S. N. Fisher, H. Godfrin, and G. R. Pickett, Nature **382**, 332 (1996).
[13] V. M. H. Ruutu, V. B. Eltsov, A. J. Gill, T. W. B. Kibble, M. Krusius, Y. G. Makhlin, B. Placais, G. E. Volovik, and W. Xu, Nature **382**, 334 (1996).
[14] M. W. Ray, E. Ruokokoski, S. Kandel, M. Möttönen, and D. S. Hall, Nature **505**, 657 (2014).
[15] M. W. Ray, E. Ruokokoski, K. Tiurev, M. Möttönen, and D. S. Hall, Science **348**, 544 (2015).
[16] C. M. Savage and J. Ruostekoski, Phys. Rev. A **68**, 043604 (2003).
[17] V. Pietilä and M. Möttönen, Phys. Rev. Lett. **103**, 030401 (2009).
[18] E. Ruokokoski, V. Pietilä, and M. Möttönen, Phys. Rev. A **84**, 063627 (2011).
[19] H. T. C. Stoof, E. Vliegen, and U. Al Khawaja, Phys. Rev. Lett. **87**, 120407 (2001).
[20] J. Ruostekoski and J. R. Anglin, Phys. Rev. Lett. **91**, 190402 (2003).
[21] A. E. Leanhardt, Y. Shin, D. Kielpinski, D. E. Pritchard, and W. Ketterle, Phys. Rev. Lett. **90**, 140403 (2003).
[22] L. S. Leslie, A. Hansen, K. C. Wright, B. M. Deutsch, and N. P. Bigelow, Phys. Rev. Lett. **103**, 250401 (2009).
[23] J.-y. Choi, W. J. Kwon, and Y.-i. Shin, Phys. Rev. Lett. **108**, 035301 (2012).
[24] J.-y. Choi, W. J. Kwon, M. Lee, H. Jeong, K. An, and Y.-i. Shin, New J. Phys. **14**, 053013 (2012).
[25] S. W. Seo, S. Kang, W. J. Kwon, and Y.-i. Shin, Phys. Rev. Lett. **115**, 015301 (2015).
[26] J. Lovegrove, M. O. Borgh, and J. Ruostekoski, Phys. Rev. A **86**, 013613 (2012).
[27] M. M. Salomaa and G. E. Volovik, Rev. Mod. Phys. **59**, 533 (1987).
[28] D. Vollhardt and P. Wölfle, *The Superfluid Phases of Helium 3* (Taylor & Francis Ltd, London, UK, 1990).
[29] Y. Kondo, J. S. Korhonen, M. Krusius, V. V. Dmitriev, Y. M. Mukharsky, E. B. Sonin, and G. E. Volovik, Phys. Rev. Lett. **67**, 81 (1991).
[30] See Supplemental Material.
[31] E. Witten, Nuclear Physics B **249**, 557 (1985).
[32] E. Radu and M. S. Volkov, Phys. Rep. **468**, 101 (2008).
[33] N. Manton and P. Sutcliffe, *Topological Solitons* (Cambridge University Press, 2004).
[34] J. Ruostekoski and J. R. Anglin, Phys. Rev. Lett. **86**, 3934 (2001).
[35] R. A. Battye, N. R. Cooper, and P. M. Sutcliffe, Phys. Rev. Lett. **88**, 080401 (2002).
[36] C. M. Savage and J. Ruostekoski, Phys. Rev. Lett. **91**, 010403 (2003).
[37] J. Ruostekoski, Phys. Rev. A **70**, 041601 (2004).
[38] T. Kawakami, T. Mizushima, M. Nitta, and K. Machida, Phys. Rev. Lett. **109**, 015301 (2012).
[39] U. Al Khawaja and H. Stoof, Nature **411**, 918 (2001).
[40] S. B. Gudnason and M. Nitta, Phys. Rev. D **90**, 085007 (2014).
[41] D. Tong, Phys. Rev. D **69**, 065003 (2004).
[42] M. Nitta and W. Vinci, Nucl. Phys. B **848**, 121 (2011).
[43] M. Eto, Y. Isozumi, M. Nitta, K. Ohashi, and N. Sakai, J.Phys. **A39**, R315 (2006).
[44] M. Shifman and A. Yung, Rev. Mod. Phys. **79**, 1139 (2007).
[45] Y. Kawaguchi and M. Ueda, Phys. Rep. **520**, 253 (2012).
[46] S.-K. Yip, Phys. Rev. Lett. **83**, 4677 (1999).
[47] U. Leonhardt and G. Volovik, JETP Lett. **72**, 46 (2000).
[48] T. Isoshima and K. Machida, Phys. Rev. A **66**, 023602 (2002).
[49] T. Kita, T. Mizushima, and K. Machida, Phys. Rev. A **66**, 061601 (2002).
[50] T. Mizushima, K. Machida, and T. Kita, Phys. Rev. Lett. **89**, 030401 (2002).
[51] J.-P. Martikainen, A. Collin, and K.-A. Suominen, Phys. Rev. A **66**, 053604 (2002).
[52] J. W. Reijnders, F. J. M. van Lankvelt, K. Schoutens, and N. Read, Phys. Rev. A **69**, 023612 (2004).
[53] E. J. Mueller, Phys. Rev. A **69**, 033606 (2004).
[54] H. Saito, Y. Kawaguchi, and M. Ueda, Phys. Rev. Lett. **96**, 065302 (2006).
[55] A.-C. Ji, W. M. Liu, J. L. Song, and F. Zhou, Phys. Rev. Lett. **101**, 010402 (2008).
[56] M. Takahashi, V. Pietilä, M. Möttönen, T. Mizushima, and K. Machida, Phys. Rev. A **79**, 023618 (2009).
[57] S. Kobayashi, Y. Kawaguchi, M. Nitta, and M. Ueda,

Phys. Rev. A **86**, 023612 (2012).
[58] M. O. Borgh and J. Ruostekoski, Phys. Rev. Lett. **109**, 015302 (2012).
[59] J. Lovegrove, M. O. Borgh, and J. Ruostekoski, Phys. Rev. Lett. **112**, 075301 (2014).
[60] S. Knoop, T. Schuster, R. Scelle, A. Trautmann, J. Appmeier, M. K. Oberthaler, E. Tiesinga, and E. Tiemann, Phys. Rev. A **83**, 042704 (2011).
[61] Y. G. Rubo, Phys. Rev. Lett. **99**, 106401 (2007).
[62] K. G. Lagoudakis, T. Ostatnický, A. V. Kavokin, Y. G. Rubo, R. André, and B. Deveaud-Plédran, Science **326**, 974 (2009).
[63] M. Kleman and O. D. Lavrentovich, *Soft Matter Physics: An Introduction* (Springer, New York, 2003).
[64] M. R. Matthews, B. P. Anderson, P. C. Haljan, D. S. Hall, C. E. Wieman, and E. A. Cornell, Phys. Rev. Lett. **83**, 2498 (1999).
[65] M. O. Borgh and J. Ruostekoski, Phys. Rev. A **87**, 033617 (2013).
[66] J. Javanainen and J. Ruostekoski, J. Phys. A Mat. Gen. **39**, L179 (2006).
[67] F. Gerbier, A. Widera, S. Fölling, O. Mandel, and I. Bloch, Phys. Rev. A **73**, 041602 (2006).
[68] J. Guzman, G.-B. Jo, A. N. Wenz, K. W. Murch, C. K. Thomas, and D. M. Stamper-Kurn, Phys. Rev. A **84**, 063625 (2011).
[69] L. Santos, M. Fattori, J. Stuhler, and T. Pfau, Phys. Rev. A **75**, 053606 (2007).
[70] M. M. Salomaa and G. E. Volovik, Phys. Rev. Lett. **51**, 2040 (1983).
[71] M. M. Salomaa and G. E. Volovik, Phys. Rev. Lett. **56**, 363 (1986).
[72] E. V. Thuneberg, Phys. Rev. Lett. **56**, 359 (1986).
[73] W. Zhang, S. Yi, and L. You, New J. Phys. **5**, 77 (2003).
[74] J. Ruostekoski and Z. Dutton, Phys. Rev. A **76**, 063607 (2007).
[75] V. R. Chechetkin, Zh. Eksp. Teor. Fiz **71**, 1463 (1976).
[76] P. W. Anderson and G. Toulouse, Phys. Rev. Lett. **38**, 508 (1977).
[77] A. E. Leanhardt, A. Görlitz, A. P. Chikkatur, D. Kielpinski, Y. Shin, D. E. Pritchard, and W. Ketterle, Phys. Rev. Lett. **89**, 190403 (2002).
[78] Y. Shin, M. Saba, M. Vengalattore, T. A. Pasquini, C. Sanner, A. E. Leanhardt, M. Prentiss, D. E. Pritchard, and W. Ketterle, Phys. Rev. Lett. **93**, 160406 (2004).
[79] M. F. Andersen, C. Ryu, P. Cladé, V. Natarajan, A. Vaziri, K. Helmerson, and W. D. Phillips, Phys. Rev. Lett. **97**, 170406 (2006).
[80] T. H. R. Skyrme, Proc. R. Soc. London A **260**, 127 (1961).